

MICROCOPY RESOLUTION TEST CHART
NATIONAL BUREAU OF STANDARDS-1963-A

12

AFGL-TR-83-0059

LARGE SPACE INSTRUMENTATION TO MEASURE
THE INTERACTION BETWEEN SPACE STRUCTURES
AND THE ENVIRONMENT

Ching-I. Meng

Applied Physics Laboratory
Johns Hopkins Road
Laurel, Maryland 20707

Final Report
1 October 1981 - 30 September 1982

December 1982

Approved for public release; distribution unlimited.

AIR FORCE GEOPHYSICS LABORATORY
AIR FORCE SYSTEMS COMMAND
UNITED STATES AIR FORCE
HANSCOM AFB, MASSACHUSETTS 01731

83 07 6 208

DTIC
ELECTE
JUL 7 1983
S
A
B
D

DTIC FILE COPY ADA129990

Qualified requestors may obtain additional copies from the Defense Technical Information Center. All others should apply to the National Technical Information Service.

UNCLASSIFIED

SECURITY CLASSIFICATION OF THIS PAGE (When Data Entered)

REPORT DOCUMENTATION PAGE		READ INSTRUCTIONS BEFORE COMPLETING FORM
1. REPORT NUMBER AFGL-TR-83-0059	2. GOVT ACCESSION NO. A129990	3. RECIPIENT'S CATALOG NUMBER
4. TITLE (and Subtitle) Large Space Instrumentation to Measure the Interaction Between Space Structures and the Environment	5. TYPE OF REPORT & PERIOD COVERED Final 10/1/81-9/30/82	
	6. PERFORMING ORG. REPORT NUMBER	
7. AUTHOR(s) Ching-I. Meng	8. CONTRACT OR GRANT NUMBER(s) MIPR No. FY71218200007	
9. PERFORMING ORGANIZATION NAME AND ADDRESS Applied Physics Laboratory The Johns Hopkins University Laurel, Maryland 20707	10. PROGRAM ELEMENT, PROJECT, TASK AREA & WORK UNIT NUMBERS P.E. 62101F 766110AC	
11. CONTROLLING OFFICE NAME AND ADDRESS Air Force Geophysics Laboratory Hanscom AFB, Massachusetts 01731 Monitor/Dr. R.P. Vancour/PHK	12. REPORT DATE December 1982	
	13. NUMBER OF PAGES 17	
14. MONITORING AGENCY NAME & ADDRESS (if different from Controlling Office)	15. SECURITY CLASS. (of this report) Unclassified	
	15a. DECLASSIFICATION/DOWNGRADING SCHEDULE	
16. DISTRIBUTION STATEMENT (of this Report) Approved for public release; distribution unlimited.		
17. DISTRIBUTION STATEMENT (of the abstract entered in Block 20, if different from Report)		
18. SUPPLEMENTARY NOTES		
19. KEY WORDS (Continue on reverse side if necessary and identify by block number) Large Space Structure and Environment Interaction		
20. ABSTRACT (Continue on reverse side if necessary and identify by block number) The major effort at the Applied Physics Laboratory of the Johns Hopkins University while participating in the Air Force Geophysics Laboratory's planning of the polar orbiting space shuttle payload definition is to provide necessary information on the polar region space environment and suggestions on the various measurements of the interaction between the space structure and the environment. During the first phase, the effort was concentrated on the polar region space environment, and results of the investigation were presented		

UNCLASSIFIED

SECURITY CLASSIFICATION OF THIS PAGE(When Data Entered)

20. to the first meeting of the IMPS Definition Phase at JPL. During the second phase of the program, the major effort was on the investigation of possible instrumentation to perform measurements of the interaction between space structures and the environment. Four measurements and their instrumentation were conceived and suggested to the IMPS Definition Team. These are summarized here.

A.

UNCLASSIFIED

SECURITY CLASSIFICATION OF THIS PAGE(When Data Entered)

FOREWORD

The work described in this report was carried out under contract to the Air Force Geophysics Laboratory, Hanscom Air Force Base, Massachusetts. The Contract Monitor was Dr. Roger P. Vancour of the Spacecraft Environment Branch, Space Physics Division.



Proposed by		✓
Reviewed by		
Approved by		
Date		
Distribution		
Availability		AS
Dist	Special	
A		

TABLE OF CONTENTS

	<u>Page</u>
FOREWORD	111
1. INTRODUCTION	1
2. STUDY OF THE INTERACTION BETWEEN UPPER ATMOSPHERIC MOLECULES AND SATELLITE SURFACES	1
3. INSTRUMENTED BOOM EXPERIMENT (IBEX)	2
4. SPACE CHARGE MEASUREMENT	2
5. THE THREE AXIS, ARC SECOND PRECISION ATTITUDE TRANS- FER SYSTEM	3
6. APPENDIX 1	5
7. APPENDIX 2	9

1. INTRODUCTION

The major effort at the Applied Physics Laboratory of The Johns Hopkins University while participating in the Air Force Geophysics Laboratory's planning of the polar orbiting space shuttle payload definition is to provide necessary information on the polar region space environment and suggestions on the various measurements of the interaction between the space structure and the environment. During the first phase (see Status Report No. 1), our effort was concentrated on the polar region space environment, and results of the investigation were presented to the first meeting of the IMPS Definition Phase at JPL.

During the second phase of the program, our major effort was on the investigation of possible instrumentation to perform measurements of the interaction between space structures and the environment. Four measurements and their instrumentation were conceived and suggested to the IMPS Definition Team. These are summarized here.

2. STUDY OF THE INTERACTION BETWEEN UPPER ATMOSPHERE MOLECULES AND SATELLITE SURFACES

The study of upper atmospheric density and the prediction of satellite drag forces is hampered by lack of understanding of the nature of the interaction between atmosphere molecules and satellite surfaces. To establish which mechanism is operating, it is proposed that sensitive measurements be made of the relative variation of drag coefficient with incident angle on flat plates.

A pair of plates, possibly of different materials, with adjustable incident angles will be mounted on opposite sides of a sensitive torsional balance. The plates will be exposed to the incident atmospheric stream. One plate will be rotated to a desired incident angle, and shutters shielding the other plate will be moved to adjust the area of it which is exposed. In this way, the balance will be steered to the null position. Drag coefficient variation with incident angle and surface material can thus be measured without knowledge of atmospheric density. The accuracy of the experiment will be

great enough to establish which molecule-surface interaction mechanism is operating. The instrument would then be usable in the non-null mode to measure atmospheric density directly.

A reprint on the concept of this experiment is enclosed as Appendix 1.

3. INSTRUMENTED BOOM EXPERIMENT (IBEX)

The Instrumented Boom Experiment is proposed for the purpose of demonstrating the feasibility of erecting a long, rigid graphite-epoxy structure in space, and for the purpose of measuring its static and dynamic properties in the polar orbital environment.

An erectable truss consisting of tapered graphite epoxy members with precise fitting snap-together aluminum joints will be fabricated. In orbit, astronauts will assemble this structure during an Extra-Vehicular Activity (EVA) period. It will consist of a boom between 20 and 100 meters long, and will be cantilevered from the shuttle cargo bay. A taut-wire sensor system (new technology developed at APL) will be used to instrument the boom, so that deformations can be accurately measured to high precision. Boom static deformations, structural rigidity, and dynamic properties will be investigated under conditions of varying atmospheric density (due to the polar orbit), insulation, and mechanical forces due to shuttle orbiter thruster firings. All data will be recorded aboard the shuttle for later processing on the ground, and the boom will be abandoned in orbit at the conclusion of the experiment.

Alternatively, a free flying deployment could be used through the addition of a maneuvering, attitude-control, telemetering package.

4. SPACE CHARGE MEASUREMENT

(a) It is proposed that a small, low power, lightweight, instrumentation package, based on the vibrating reed electrometer principle for non-contact measurement of the static electric field normal to a conducting surface, be

developed and qualified for space use. This package would be a general purpose instrument which could be used in the investigation of spacecraft charging phenomena.

(b) The electrometer developed above should be attached to a spacecraft to measure surface charge or ambient electric field. This task would include developing interfaces to spacecraft power and data storage systems. Further, it would be desirable to collaborate with an investigator who would develop an analytical or numerical model for this experiment.

(c) Charge particle detectors should be added to investigate charge build-up on the surface of a satellite in relation to ambient radiation. It would be desirable to collaborate with another investigator who would develop the analytical or numerical model for this experiment.

(d) The electrometer should be used to investigate charge build-up as an isolated body within a spacecraft in relation to ambient radiation. This would require charge particle detectors. The isolated body would be a cylinder supported by magnetic repulsion in the manner of the discos proof mass. The rod carrying the suspension current might be oriented perpendicular to the direction of satellite travel. It should be possible to design the configuration to eliminate the need for thrusters to keep the cylindrical proof mass in position.

5. THE THREE AXIS, ARC SECOND PRECISION ATTITUDE TRANSFER SYSTEM

Frequently, an instrumental package is located on a long boom extension away from the body of the spacecraft for various reasons. Therefore, it is sometimes essential to know the precision measurement of the instrument package attitude relative to the spacecraft main attitude sensors (such as star cameras). A three-axis attitude transfer system developed at APL/JHU is able to provide a measure of the relative attitude change between the spacecraft and the boom. This system can also be used to measure the degree of the deformation for the space structure components.

A common mounting structure is provided for the spacecraft stellar sensors (or the main space structure) and the optical auto-collimation transceivers of this Attitude Transfer System (ATS) in the form of a specially designed graphic fibre epoxy optical bench. This system is capable of measuring the variation along three axes (pitch, yaw and roll better than 3 arc seconds (i.e., 1.5×10^{-5} rad). This 3-axis, high precision attitude transfer system can be used to monitor the deformation (including vibration and twist of any component of a large space structure).

A reprint on a similar system is enclosed as Appendix 2.

APPENDIX 1

**The Drag Balance: An Apparatus for Studying
Atmosphere-Satellite Surface Interactions**

by

A. D. Goldfinger



The Drag Balance: An Apparatus for Studying Atmosphere-Satellite Surface Interactions

A.D. Goldfinger

Reprinted from

Journal of Spacecraft and Rockets

Volume 17, Number 6, Nov-Dec 1980, Page 565.
Copyright American Institute of Aeronautics and Astronautics, Inc., 1980. All
rights reserved.

The U.S. Government is authorized to reproduce and sell this report.
Permission for further reproduction by others must be obtained from
the copyright owner.

AMERICAN INSTITUTE OF AERONAUTICS AND ASTRONAUTICS • 1290 AVENUE OF THE AMERICAS • NEW YORK, NEW YORK, N.Y. 10104

The Drag Balance: An Apparatus for Studying Atmosphere-Satellite Surface Interactions

Andrew D. Goldfinger*

The Johns Hopkins University Applied Physics Laboratory, Laurel, Md.

THE interaction between upper atmosphere molecules and satellite surfaces is poorly understood. Because of this, accurate theoretical determination of drag coefficients is not currently possible. Since the drag force on a surface is dependent on the product of drag coefficient and atmospheric density, this inaccuracy in drag coefficient prediction also limits the accuracy with which atmospheric density can be deduced from measurements of satellite drag.¹

Study of this interaction has produced a large volume of literature, but the difficulty of duplicating orbital conditions in the laboratory has hampered the acquisition of high-quality experimental data. Theoretical studies have yielded models that are rather general, and depend upon a number of parameters, such as that due to Schamberg,² but it has proven difficult to determine values of these parameters due to the lack of relevant experimental data.

The models of Schamberg and others show that the drag coefficient on a flat plate as a function of incident angle has a shape dependent on the values of the parameters. Hence, a precise measurement of the relative drag coefficients at varying incident angles on a flat plate of given material would enable the values of these coefficients to be determined for this material.

This observation has led to the concept of the experiment described below. It employs a sensitive torsional balance to measure the relative variation of drag coefficient on a flat plate with incident angle, and the configuration is such that the measurement is not dependent upon knowledge of atmospheric density. Torsional balances have been used before in molecule-surface interaction studies,³ but not with incident particle energies as great as those in orbit, nor in the configuration proposed here.

Consider a flat plate of area A whose surface normal makes an angle θ to the incoming atmospheric beam. The atmosphere has density ρ and speed V . The drag force on the plate will be given by

$$F_D = \frac{1}{2} \rho V^2 A \cos \theta C_D(\theta, i) \quad (1)$$

where $C_D(\theta, i)$ is the drag coefficient for a plate of material i at incident angle θ . Equation (1) is actually the definition of the drag coefficient.

To infer C_D from measurements of F_D it is necessary to know ρ and V . The latter quantity is readily available, but the

atmospheric density is highly variable. Hence, the following approach is taken.

A torsional balance is constructed as shown in Fig. 1. Two plates, whose surfaces are coated with materials i and j , are mounted on the balance. One is fixed at normal incidence to the incoming atmospheric beam, and the other is free to rotate so that its incident angle can be changed. The rotation axis is along the arm of the balance so that any lift forces generated by the rotatable plate will not torque the balance in the direction in which it is free to move. Movable shutters attached to the spacecraft frame are positioned in front of the fixed plate to adjust the area of it exposed to the atmospheric beam.

To perform the experiment, the movable plate is first rotated to a selected incident angle θ . Then, the shutters are adjusted until the balance arm comes to the initial "zero" position, where the forces on the two plates are equal. The equation representing this condition is

$$\frac{1}{2} \rho V^2 A \cos \theta C_D(\theta, i) = \frac{1}{2} \rho V^2 a(\theta) C_D(0, j) \quad (2)$$

where $a(\theta)$ is the area exposed by the shutters when the balance is nulled with the movable plate at angle θ . From Eq. (2),

$$C_D(\theta, i) / C_D(0, j) = a(\theta) / A \cos \theta \quad (3)$$

The quantities on the right are known, so the ratio on the left, which is the relative variation of drag coefficient with incident angle, can be determined with no knowledge of atmospheric density.

By choosing both plates of the same material, the functions $C_D(\theta, i)$ can be determined to within a multiplicative constant. By interchanging plates of different materials, the various $C_D(\theta, i) / C_D(0, j)$ ratios can be measured. Other balance configurations can be chosen to compare the lift forces on two plates, or even the lift force on one plate with the drag force on another.

Thus the drag balance concept shows promise of significantly improving understanding of molecule-surface interactions. It is next necessary to demonstrate its feasibility.

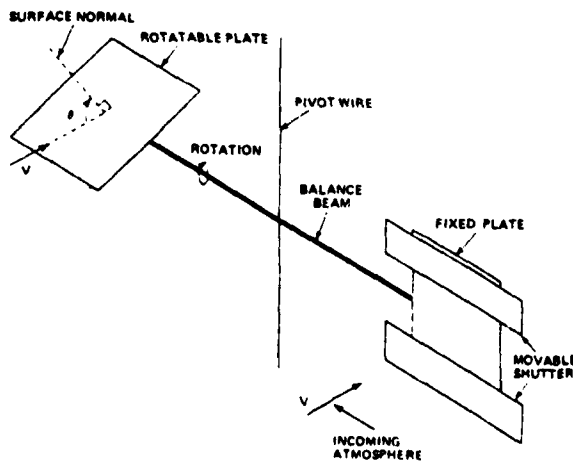


Fig. 1 Drag balance concept.

Received March 24, 1980; revision received Aug. 18, 1980. Copyright © American Institute of Aeronautics and Astronautics, Inc., 1980. All rights reserved.

Index categories: Rarefied Flows; Atmospheric and Space Sciences.

*Physicist, Space Department.

Assume each drag plate has an area A and mass/area density σ . If the balance beam is of length $2D$ and its mass is negligible, the moment of inertia is

$$I = 2\sigma AD^2 \quad (4)$$

Let P_D be the drag pressure (force per unit area) on each plate. The torque due to the full area of the fixed plate will be

$$\tau_0 = AP_D D \quad (5)$$

To be able to measure the drag force to a fractional precision ϵ , the system should be capable of sensing a net torque of

$$\delta\tau = \epsilon\tau_0 = \epsilon AP_D D \quad (6)$$

Let the torsional constant of the pivot wire be K . The balance must be adjustable to the null position to within an angle

$$\delta\phi = \delta\tau/K = \epsilon AP_D D/K \quad (7)$$

To maximize sensitivity, $\delta\phi$ should be as large as possible.

The actual nulling of the balance, by adjustment of the shutter aperture σ , is done by a control loop. This loop must have the capability of steering the balance to the null position with zero steady-state error in a time short enough to allow measurements to be completed quickly. One such loop has been designed that settles the balance to the null position to within 0.1% of the input step magnitude in a time equal to

$$T_{0.1\%} = 27.6\sqrt{I/K} \quad (8)$$

Based upon these computations, a study has demonstrated the feasibility of the experiment. It has shown that a balance can be designed that is sensitive enough to distinguish between the molecule surface interaction mechanisms of interest, yet is responsive enough to allow measurements to be made in a relatively short time.

Four interaction mechanisms were considered. Of these, the hardest to distinguish were the thermal re-emission and the total-absorption models. It was determined that measurement of the relative drag force with an accuracy of 0.1% would allow these interaction mechanisms to be distinguished, hence

$$\epsilon = 10^{-3} \quad (9)$$

was chosen as the required fractional measurement precision of the apparatus.

The study showed that this precision is possible in a balance capable of performing measurements at 5-min. intervals if the drag plates are made of aluminum foil with a surface mass density of $\sigma = 0.01 \text{ gm/cm}^2$, and the balance arms are $D = 5 \text{ cm}$ long. A zero-gravity taut band suspension system would be used with a torsional constant of $K = 0.035 \text{ dyne cm/rad}$.

A number of technical concerns remain. These include the following.

1) To prevent interference from the cloud of emitted and scattered molecules surrounding the spacecraft, the experiment must be deployed at the end of a boom. This cloud of molecules must be studied and modeled to determine the required boom length and the seriousness of the interference.

2) The shutter will have to be mounted so that "fringing" of the atmospheric beam due to thermal motion does not change the effective area. The trapping of molecules between the shutter and drag plate will also have to be eliminated. If this is impractical, an alternative approach is to dispense with the shutters altogether and allow the area of the fixed plate to vary by other means, such as using two movable overlapping plates.

3) Sun and albedo shields must be designed to remove the effects of radiation pressure.

4) Means must be provided to prevent forces due to charge buildup. At the least, the entire balance system will have to be grounded.

5) A more optimal control loop must be designed.

6) The possibility of resonance between the balance beam and spacecraft attitude excursions must be eliminated.

7) Active temperature control may be necessary.

Acknowledgments

This work was supported by the Department of the Navy under Contact N00024-78-C-5384 with the Applied Physics Laboratory of The Johns Hopkins University.

References

- ¹Imbro, D.R. and Moe, M.M., "On Fundamental Problems in the Deduction of Atmospheric Densities from Satellite Drag," *Journal of Geophysical Research*, Vol. 80, Aug. 1975, p. 3077.
- ²Schamberg, R., "A New Analytic Representation of Surface Interaction for Hyperthermal Free Molecular Flow with Application to Neutral-Particle Drag Estimates of Satellites," Rand Corporation Report No. RM-2313, Jan. 1959.
- ³Schmidt, C. and Schiff, H.E., "Accommodation Coefficient Measurements with a Sensitive Torsion Balance," *Review of Scientific Instruments*, Vol. 42, April 1971, p. 442.

APPENDIX 2

The MAGSAT Three-Axis Arc Second Precision Attitude Transfer
System

by

F. W. Schenkel and R. J. Heins

THE MAGSAT THREE AXIS ARC SECOND PRECISION ATTITUDE TRANSFER SYSTEM

F. W. SCHENKEL and R. J. HEINS

The Johns Hopkins University, Applied Physics Laboratory, Laurel, Maryland 20810, USA

The MAGSAT spacecraft, the purpose of which was to perform a precision mapping of the Earth's magnetic field, required highly sophisticated instrumentation to accomplish its mission objectives. Both a scaler and a three-axis vector magnetometer package were employed to make precise magnetic field measurements. Conducting such magnetic measurements also requires a precise satellite navigation capability as well as a very precise knowledge of the three-axis attitude of the magnetometer instrument package. This paper addresses the precision measurement of the instrument package attitude relative to a pair of star camera spacecraft attitude sensors. Because of the need for magnetic cleanliness in the immediate area of the magnetometer instrument package, it was necessary to separate these instruments from the main body of the spacecraft via a 20 ft long scissors boom extension. The inherent magnetic properties of the star camera sensors demanded that they be secured to the spacecraft body. A three axis attitude transfer system was therefore created to provide a measure of the relative attitude change between the magnetometer package and the stellar sensors. A common mounting structure was provided for the stellar sensors and the optical autocollimation transceivers of the Attitude Transfer System (ATS) in the form of a specially designed graphic fibre epoxy optical bench.

The design principles, performance characteristics and testing of the integrated system are described in this paper. The standard error in the integrated system attitude was within ± 3 arc seconds for all three axis.

1. BACKGROUND

THE MAGSAT SPACECRAFT was designed to provide precision magnetic survey mapping to an accuracy of six γ * of the whole Earth from a polar, Sun synchronous orbit. A precise knowledge of the attitude of the vector magnetometer instrument relative to a precisely defined geocentric reference system was required. A precise knowledge as to where the magnetometer instrument was viewing the Earth was accomplished by referencing the vector magnetometer coordinate axes to the coordinate axes as defined by a set of star mapping cameras. The local spacecraft magnetic contamination had to be less than one γ ; therefore, the magnetometer instrument was attached to a specially designed platform of graphite fibre

material remotely suspended from the spacecraft body via a 20 ft long extendable boom also made of graphite fibre material. The star cameras (being highly magnetic) were located on the spacecraft body. This remote instrument location established a need for precision attitude transfer in Pitch, Yaw and Roll between the remote vector magnetometer instrument and the star cameras. Therefore, the ATS (Attitude Transfer System), which is the essence of this paper, was born. Figure 1 illustrates the general design layout of the MAGSAT. The ultimate total system accuracy was dependent upon the thermo-mechanical integrity of the "Optical Bench" which served as a common mounting platform for the attitude transfer system and the star sensor cameras.

* 1 γ = 10^{-5} Oersted.

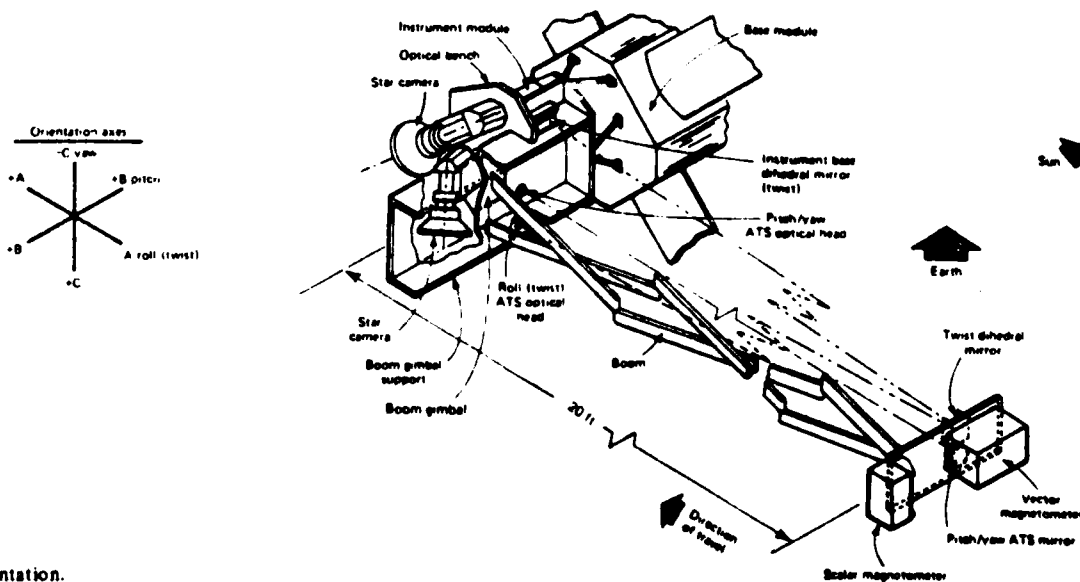


Fig. 1. ATS orientation.

TABLE 1. Attitude Transfer System Operational Characteristics.

Accuracy:	
Pitch/Yaw	5 arc seconds
Roll	5 arc seconds
Dynamic Range:	
Acquisition	± 6 arc min simultaneous with Pitch/yaw
	± 1 inch displacement
Precision Linear Range	
Pitch/Yaw	± 3 arc minutes ± 0.75 inch displacement
Roll	± 5 arc minutes
Thermo-Mechanical Interface Stability	
Glint Immunity	
Pulsed GaAs Led at 9300 Å	
Narrow Band Filter	
Synchronous Demodulation	
Automatic Gain Control	
Data Rate (3 Axis) 10 Per Second (Max)	
Weight:	15.35 lb
Power:	3½ W

2. GENERAL

The ATS system was designed, built and flown utilizing two highly sophisticated autocollimators. The system design theory and operation is described in the following sections.

2.1 ATS Characteristics

The ATS functioned with a 20 ft long boom over a dynamic range in magnetometer platform displacement motion of ± 0.25 degrees in any transverse direction. The twist motion dynamic range was to be a minimum of ± 0.083 degrees.

The attitude transfer system operational characteristics are summarized in Table 1. The ATS was designed to permit precision performance in a totally solar illuminated environment via an optically narrow banded system with synchronous demodulation at a wavelength of 9300 Å. Immunity to glint from other spacecraft components was demonstrated in a series of spoofing attempts.

3. DESIGN THEORY

The described design concept for a precision attitude transfer system is predicated upon proven autocollimation techniques. All active components were located on the satellite body. The magnetometer instrument platform was equipped with two passive optical reflectors. There were no moving components. The pitch and yaw axes angle measurements were performed by a common optical transceiver in conjunction with a flat mirror at the magnetometer instrument platform. The roll axis angular measurement utilized a double pass optical system having an optical transceiver plus a dihedral mirror located at the spacecraft optical bench and working in conjunction with a remote dihedral mirror at the magnetometer instrument platform. This is shown in Fig. 1. The flat mirror, in conjunction with the pitch/yaw optics head, was used to generate analog and digital pitch/yaw signals proportional to actual pitch and yaw. In like fashion, the remote dihedral mirror operating in conjunction with the roll optics head and the base dihedral mirror (also mounted on the optics bench) generated an analog and digital roll signal proportional to the roll axis attitude ('twist' of boom end mass relative to roll optics head).

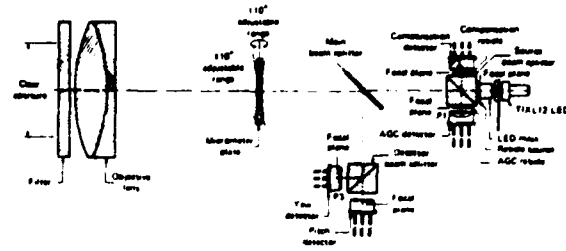


Fig. 2. Schematic of the ATS pitch/yaw autocollimator.

3.1 Pitch/Yaw Optical Design

The pitch/yaw portion, being the less complex system, will be described first. Figure 2 illustrates in schematic form the parts of the pitch/yaw transceiver optical head. In brief, an optical signal at a wavelength of 9300 Å and pulsed at a rate of 125 Hz was derived from an LED (TI Type XL-12). This radiation passed through a square mask (LED mask) and then through a second square mask (Reticle source). The reticle source mask lay at the infinity focal plane of the objective lens. The LED mask was used to define the external pupil of the optical system at the remote flat mirror located on the magnetometer instrument platform at a distance of 20 ft. The output optical beam after leaving the reticle source passed through a 'source beam' splitter, 'main beam' splitter and then a 'micrometer plate' refractor. The micrometer plate was mounted on a two axes gimbal having precision angular control. By adjusting the angle of the micrometer plate it was possible to perform precise (arc second) steering (for calibration) of the output optical beam over a limited range of ± 3 arc minutes. The output beam then passed through the objective lens and 'optical filter' to impinge upon the remote flat mirror for auto reflection back to the pitch/yaw optical head.

The return optical beam reentered the system in the reverse direction through the narrow band (500 Å wide) interference filter, objective lens, micrometer plate and on to the main beam splitter. At the main beam splitter the return beam was divided. Part of the signal went back to the source beam splitter and the remainder to the pitch and yaw angle detectors. Before arriving at the angle detectors, however, the optical return was further split by a 'detector beam splitter.' Both the pitch and the yaw detectors lay in the return infinity focal plane of the objective lens. An image of the square transmitted 'reticle' source mask was formed at both the pitch and the yaw detectors, each consisting of a silicon diode pair. Figure 3 illustrates the superposition of the pitch and yaw detector pairs which, in effect, resulted in a quadrature system. The cross hatched area shows the return beam image. The detector geometric design permitted operation in either a nulling mode or in a constant measurement mode. The latter was used in this application.

That portion of the return optical beam going from the main beam splitter to the source beam splitter was imaged on an AGC detector which also lay on a return infinity focal plane of the objective lens. Again, this return beam image was a replica of the reticle source mask. The AGC detector was a single element silicon diode which measured the signal strength of the return optical beam with the inclusion of any possible degradation due to the optical train components or aging in the LED source. By comparison of the optical return AGC signal level with a fixed reference, a control loop governing the LED current and therefore the LED optical output level was closed. In this

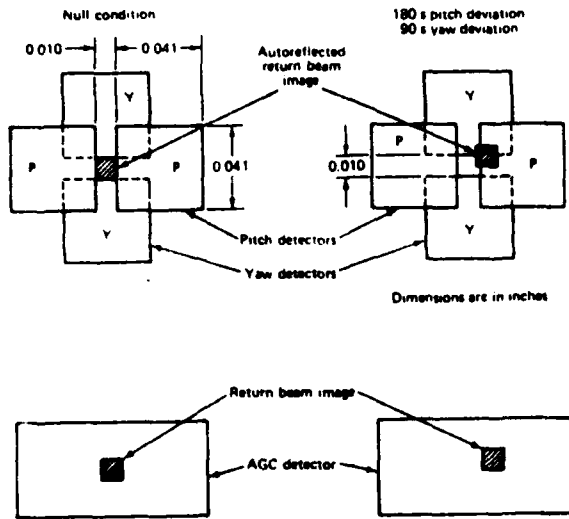


Fig. 3. Image and detector relationships in pitch/yaw system.

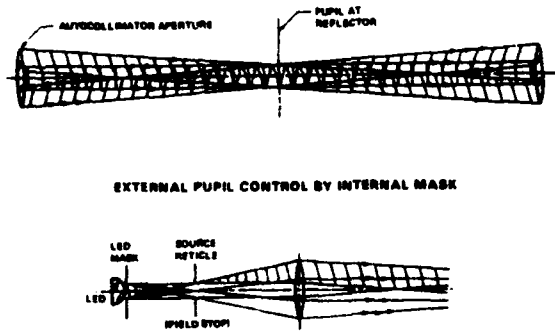


Fig. 4. External system pupil in pitch/yaw system.

manner the pitch and yaw angle detector error signals were continually normalised.

It can be seen from Fig. 2 that one additional detector, called the 'compensation detector,' was near the LED transmitter. The source beam splitter derived a small percentage of the transmit beam to impinge upon the compensation detector. There was always a small amount of scattered transmitter signal from the LED which may have reached the pitch/yaw and AGC detectors and resulted in angle measurement errors. Therefore, the compensation detector output was utilised to pick out any pitch, yaw or AGC extraneous signal regardless of the LED output optical signal level which might have been required to compensate for optical train component degradation other than the LED.

Figure 4 illustrates in a schematic ray diagram form the system optical pupil and its formation. The pupil formed at the 3 inches square remote flat mirror was approximately 0.7 inches square. This avoided severe vignetting of the return signal which might have resulted from mirror translations of greater than 1.25 inches at the end of a 20 ft long boom.

The optical/geometric angle measurement relationships for the pitch and yaw portions of the ATS are illustrated in Fig. 5. The analog output from both the pitch and the yaw angle measurement detector pairs was digitised. A discussion of the system electronics is presented in subsequent sections.

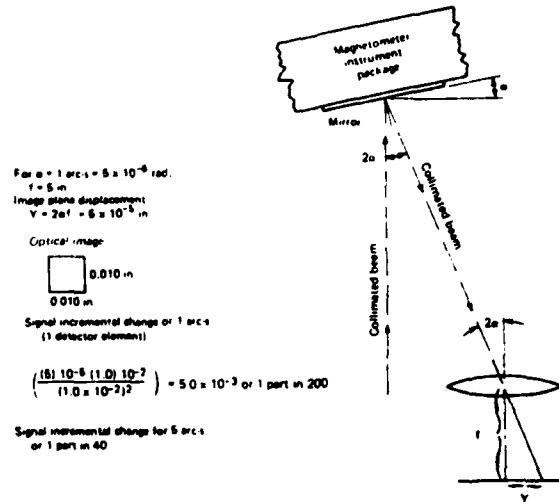


Fig. 5. Optical geometry for measuring pitch and yaw.

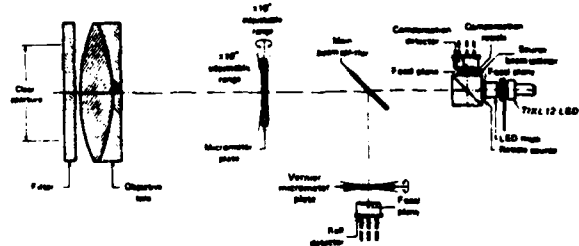


Fig. 6. Schematic of the ATS roll autocollimator.

3. 2 Roll Optical Design

The roll (twist) portion of the ATS was similar to the design of the optical transceiver head to the pitch/yaw optical transceiver head with a few exceptions. Figure 6 illustrates in schematic format the roll transceiver optical head. Figure 7 illustrates the return optical beam image and detector geometry characteristics for the roll system.

In essence, the roll angle measurement system was a pseudo yaw system as can be seen from the geometric principles illustrated in Fig. 8. If a collimated beam of light strikes a remote mirror which is at some skew angle to the beam, the reflected beam will describe a circular motion. By using a dihedral mirror as the remote reflector, the roll (twist) angle motion is decoupled from the spacecraft yaw motion. In order to also accomplish spacecraft pitch motion decoupling, a second dihedral reflector is located in the plane of the roll optical transceiver head. The MAGSAT optical bench to which the roll transceiver optical head and the base dihedral reflector were attached provided a component separation to form a base circle of 20 inches diameter. The use of a double pass (double pass denoting two passes of the optical beam at the remote dihedral reflector) optical system improved the system opto-geometric advantage by an additional factor of two and permitted consolidation of the optical transmitter and receiver into one single transceiver unit.

The optical beam striking the remote dihedral reflector was rectangular in shape since the transmitter source reticle and the LED were both rectangular. The system pupil was

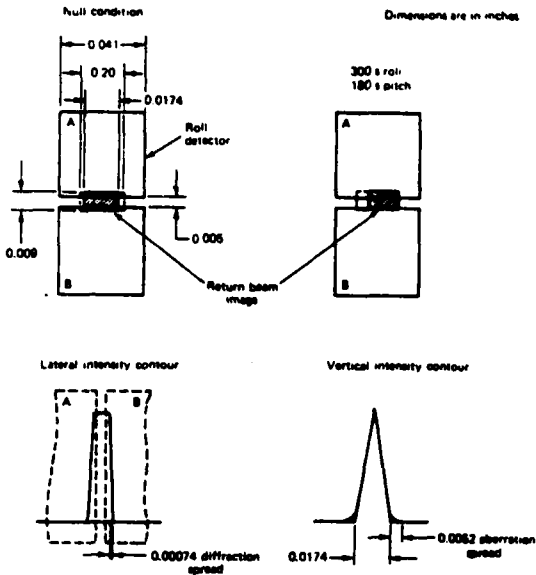


Fig. 7. Geometry of the image and detector for the roll system.

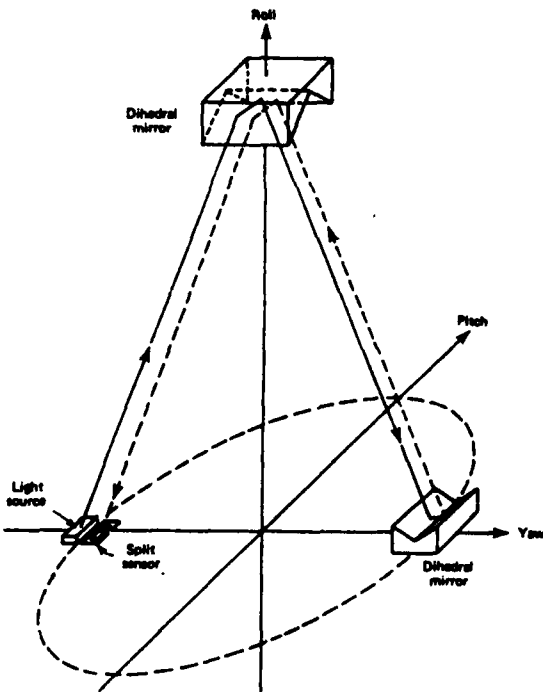


Fig. 8. Simplified diagram of the roll ATS for pitch and yaw decoupling.

located at the base dihedral reflector as shown in Fig. 9. The AB and AC planes are defined as per the spacecraft coordinate axes given in Fig. 1. The remote dihedral mirror was not precisely 90° but rather 89° 42' 24" in order to have the return optical beam reenter the transceiver optics without extreme vignetting. A detailed diagram of the ray geometry is depicted in Fig. 10.

The geometry for a collimated beam twist sensor is complex as is evident from view Fig. 10. Basically, it is the

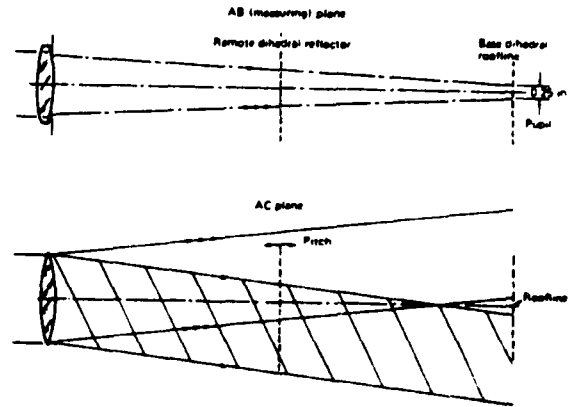


Fig. 9. Roll system in AB and AC measuring planes.

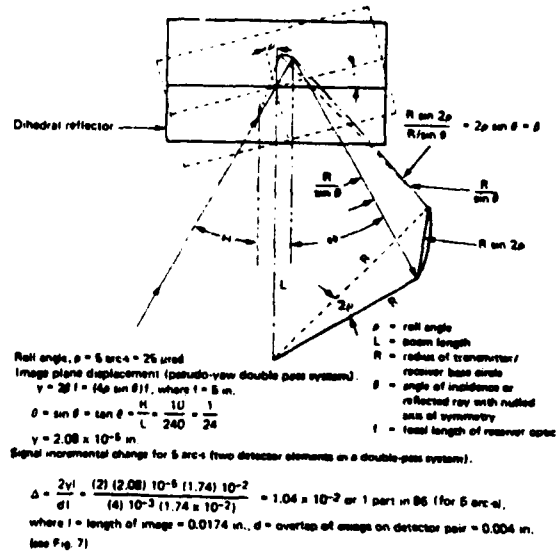


Fig. 10. Basic optical/geometric relationship for a collimated roll sensor system.

change in position of the transmitted optical image in the receiver objective optic image plane which indicates twist in the dihedral mirror fastened to the magnetometer experiment. The twist change sensitivity in the position of the image, which was split between a pair of silicon detector elements having a 0.005 inch separation, is dependent upon the beam length (L), the transmitter/receiver base circle radius (R), the focal length (FL) of the receiver optic, the linear dimension of the image and the number of passes through the system. The calculation given in Fig. 10 is indicative of the system design. A 5 arc second twist resulted in a differential receiver signal change of 1 part in 96, easily detectable.

3.3 Electro-Optics

The significant computation to be made for any of the attitude transfer is:

$$\frac{\text{Differential signal}}{\text{Noise}}$$

where the differential signal corresponds to the angular resolution capability of the particular system.

A. Pitch/Yaw Attitude Transfer System:

The ratio $\Delta Sp/Y / i_N$ is desired

where: $\Delta Sp/Y$ is the incremental signal change at the detector output.

i_N = combined noise

To compute $\Delta Sp/Y$ it is essential to include the system optical components and their transmission factors as follows:

Optical Efficiency Prognosis per Channel

Transmitter

Solid Angle LED Output Coupling	$\beta_1 = 0.05$
Aperture (LED Mask and Source Reticle)	$\beta_2 = 0.8$
Source Beam Splitter	$\beta_3 = 0.9$
Main Beam Splitter	$\beta_4 = 0.5$
Projection Objective	$\beta_5 = 0.85$
Filter	$\beta_6 = 0.90$
Mirror (at experiment)	$\beta_8 = 0.9$

Receiver

Filter	$\beta_6 = 0.9$
Objective Optic	$\beta_5 = 0.85$
Main Beam Splitter	$\beta_4 = 0.5$
Detector Beam Splitter	$\beta_7 = 0.5$
Vignetting Factor	$\beta_9 = 0.5$

Combined Optical Efficiency $E = \beta_1 \beta_2 \beta_3 \beta_4 \beta_5 \beta_6 \beta_7 \beta_8 \beta_9$

$$E = 1.17 \times 10^{-3}$$

The electrical signal level at the output of any individual channel for an edge of linear range condition may be expressed as follows (optical image totally on one detector in pair - see Fig. 3):

$$Sp/Y = P E \gamma$$

where Sp/Y = output current at detector (amps)

P = source power output (watts)

γ = detector sensitivity (amps/watt)

for a TI - XL12 IR LED source

$P = 3.2 \times 10^{-3}$ watts peak (derating at 125 Hz PRF of 0.08 to allow for aging)

for Aeroneutronic Ford Si diode detector (custom geometry)

$\gamma = 0.40$ amps/watt

for $E = 1.17 \times 10^{-3}$ (see tabulation)

$$Sp/Y = 1.51 \times 10^{-6} \text{ amps}$$

The change in signal level due to an incremental pitch or yaw change of 1 arc second is given as 1 part in 200 (see Fig. 5). Thus

$$\Delta Sp/Y = \frac{Sp/Y}{200} = \frac{1.51 \times 10^{-6}}{200} = 7.56 \times 10^{-9} \text{ amps}$$

The noise in any channel of the pitch yaw system is a combination of shot noise, detector generation-recombination noise and Johnson noise at the preamp.

Shot Noise

$$\bar{i}_{SN} = \sqrt{2e i_s (\Delta F)}$$

where \bar{i}_{SN} = RMS noise current

e = electronic charge = 1.6×10^{-19} coul

i_s = signal current

ΔF = system bandwidth at detector

if $i_s = Sp/Y$, $\Delta F = 250 \text{ Hz}^*$, then

$$\bar{i}_{SN} = 1.09 \times 10^{-11}$$

Generation-Recombination Noise

This noise is given as detector noise equivalent power NEP in watts/Hz^{1/2}. For a detector NEP = 1.4×10^{-12} W/Hz^{1/2}, and a 250 Hz bandwidth:

$$i_{GRN} = 2.2 \times 10^{-11} \text{ amps}$$

Johnson Noise

$$i_{JN} = \left[\frac{4KT(\Delta F)}{R} \right]^{1/2}$$

where K = Boltzmann Constant

= 1.38×10^{-23} watt sec/deg.

T = absolute temp K

= 300 K

R = noise resistance

1×10^9 ohms

ΔF = Bandwidth

= 2.5×10^2 Hz

$$i_{JN} = 1.17 \times 10^{-14} \text{ amps}$$

The combined noise at the detector output is given:

$$i_N = (i_{SN}^2 + i_{GRN}^2 + i_{JN}^2)^{1/2}$$

$$i_N = 2.45 \times 10^{-11} \text{ amps}$$

The noise voltage is the product of i_N and R , the load resistance.

$$V_N = 2.45 \times 10^{-11} \times 5 \times 10^9 = 1.22 \times 10^{-6} \text{ volts}$$

The noise contribution of a LM108 preamplifier is quoted as

$$v_n = 0.5 \times 10^{-6} / \text{Hz}^{1/2}$$

for $\Delta F = 2.5 \times 10^2$ Hz

$$v_n = 7.9 \times 10^{-6} \text{ volts}$$

The amplifier noise is negligible in comparison to the other sources.

The value of $\Delta Sp/Y / i_N$ can now be computed:

$$\frac{\Delta Sp/Y}{i_N} = 3.08 \times 10^2 \text{ (for 1 arc second)}$$

* The actual processing bandwidth of the modulated signal is 5 Hz.

or 49 dB

if viewed as a voltage ratio at the output of the LM108 pre-amp or if viewed as a current ratio at the detector output.

B. Twist (Roll) Attitude Transfer System

The computation for the twist channel is identical in nature to that for the pitch/yaw system with the exception of the optical efficiency E and the incremental signal change per angular resolution element of 1 part in 96 per detector for 5 arc seconds (see Fig. 10). The value of E is computed from the following tabulation:

Optical Efficiency Prognosis per Channel

Transmitter

Solid Angle LED Output Coupling	$\beta_1 = 0.05$
LED Mask and Source Reticle	$\beta_2 = 0.8$
Source Beam Splitter	$\beta_3 = 0.9$
Main Beam Splitter	$\beta_4 = 0.5$
Projection Objective	$\beta_5 = 0.85$
Filter	$\beta_6 = 0.90$
Remote Dihedral Mirror (2 bounces) x 2 Passes	$\beta_7 = 0.64$
Base Dihedral Mirror (2 bounces)	$\beta_8 = 0.81$

Receiver

Filter	$\beta_6 = 0.90$
Main Beam Splitter	$\beta_4 = 0.50$
Objective Optic	$\beta_5 = 0.85$
Vignetting Factor	$\beta_9 = 0.5$

Combined Optical Efficiency $E = \beta_1\beta_2\beta_3\beta_4^2\beta_5^2\beta_6^2\beta_7\beta_8\beta_9$

$E = 1.36 \times 10^{-3}$

$\Delta S_R = \frac{PE\gamma}{96} = \frac{(3.2)10^{-3}(1.36)10^{-3}(0.40)}{96}$ (see Fig. 10)

$\Delta S_R = 1.81 \times 10^{-8}$ amps

$\Delta S_R/i_N = 7.4 \times 10^2$ (for 5 arc seconds)
or 57 dB

Again, as in the pitch/yaw system, there is an adequate differential signal to noise ratio.

3.4 ATS Electronics

Figure 11 shows a block diagram of the MAGSAT ATS. Each of the roll and pitch/yaw optics head packages were mounted on the mechanically isolated optical bench; all remaining electronics were mounted in a single package on the instrument base module removed from the optics heads. Each optics head, in addition to transmitting and receiving optics components, contained electronics circuits which had to be physically close to the receive optics. Included in Fig. 11 are the transmitting LED, receive photo detect diodes and associated buffering circuits.

The outputs of the attitude detection blocks were in analog form, which in turn were digitised and output to the spacecraft telemetry system. The range of the pitch/yaw digital outputs were ± 205 arc sec with a scale factor of about 0.4 arc sec/bit. The roll digital output had a range of ± 340 arc sec with a scale factor of about 0.65 arc sec/bit.

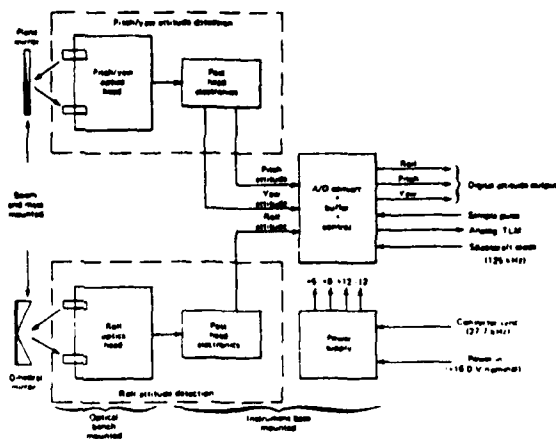


Fig. 11. Block diagram of MAGSAT ATS.

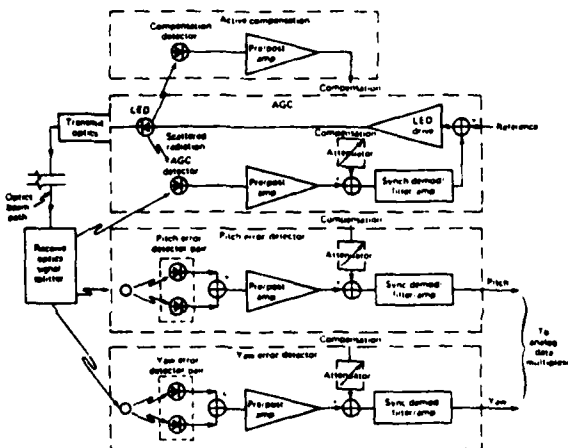


Fig. 12. Pitch/yaw channel electronics.

An A/D measurement was made on each attitude analog output four times per second.

Figure 12 gives a more detailed block diagram of the pitch/yaw attitude detection implementation.

An essential feature of attitude detection was the use of the closed loop AGC circuit. This circuit sensed the return optical signal level and generated feedback control to the LED to maintain a constant optical signal level input to the P/Y attitude detection circuit. As will be seen, this was necessary to maintain a fixed system transfer function in the presence of any changes in optical path attenuation, photodetector responsivity, LED conversion efficiency and vignetting. The circuits were designed such that at beginning of life, only about one-sixth of the maximum available LED output was used. Thus, during the life of the MAGSAT satellite, the above parameters could degrade by a combined factor of six before any significant change in system transfer functions would be experienced.

An important feature of the ATS was the use of a chopped square wave light source to allow the use of AC coupled circuits in the critical and highly sensitive front end of the attitude detection circuits to remove DC bias. Secondly, chopped light sources provide a means for minimizing any potential coupling between the roll and pitch/yaw systems. This was done by making the pulsed light sources at 125 Hz phased 90° apart. Any light leakage coupled from one system into the alternate system is 'zeroed out' due to the fact that its receiving electronics is 90° out of phase with respect to any alternate system leakage input.

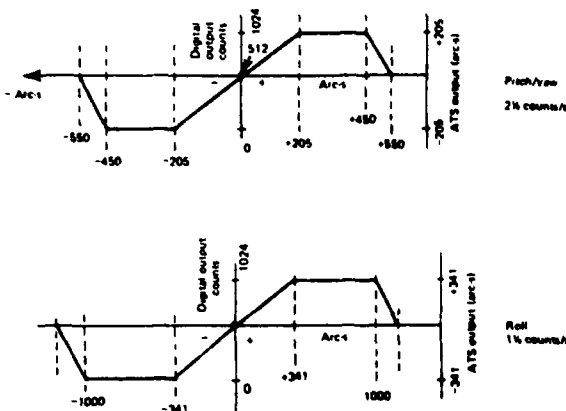


Fig. 13. ATS transfer functions (uncalibrated).

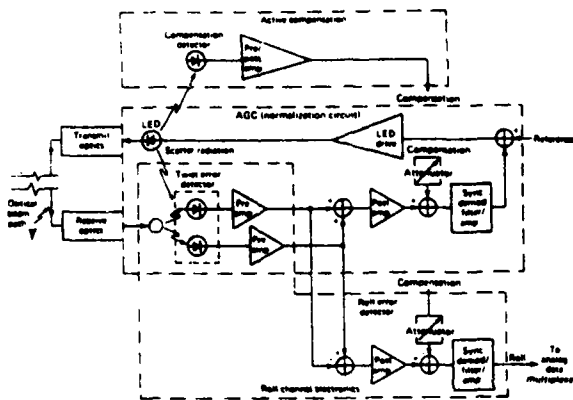


Fig. 14. Electronics implementation of roll attitude detection.

The signal was maintained in AC form through all of the buffering/scaling electronics in the pitch/yaw optics head package. The signal was then AC coupled through an RC coupling circuit with 1 Hz corner pole to a posthead buffer/amplifier located in the main electronics package. The signal was then input to a synchronous demodulator to 'rectify' the input signal to a DC level. The DC level was filtered by a 5 Hz single pole filter to smooth out any residual 125 Hz switching components.

Figure 14 shows the basic electronics implementation of roll attitude detection. From any electronics operation point of view, its operation was similar to that of the pitch and yaw attitude detection circuits.

Figure 13 also illustrates the roll system transfer function.

4. SYSTEM TEST AND PERFORMANCE

The calibration of the ATS in pitch, yaw and roll was performed by having a precision (arc second) test setup wherein the ATS optical heads and the roll system base dihedral mirror were held securely on the spacecraft optical bench while the remote vector magnetometer instrument package with the remote flat mirror and the remote dihedral mirror were mounted on a 3 axes gimbal system. This test gimbal system was rotated over, and in excess of, the required ATS performance attitude angles. The test gimbal angles were measured with the aid of a laser interferometer and a series of Kern theodolites. Simultaneously, the ATS output angles were also recorded. From this data a polynomial least

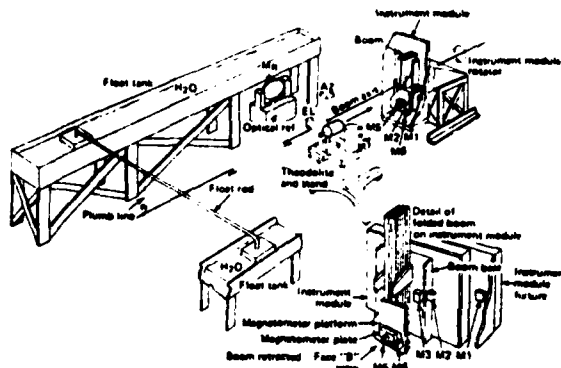


Fig. 15. Optical metrology for platform orientation of vector magnetometer plate sensors.

squares fit was established for the ATS linear operating range in each axis. These equations are as follows for the zero gravity conditions:

$$\text{Pitch} = 0.3 + 0.9877P_0 - 0.00411Y_0 - 0.00148P_0^2 + 0.000067Y_0^2 - 0.000205P_0Y_0 - 2.4 \sin(P_0/150)$$

The standard error is 2.1 arc sec for pitch.

$$\text{Yaw} = -1.5 + 0.9924Y_0 - 0.0255P_0 - 0.00015Y_0^2 + 0.00034P_0Y_0 - 1.4 \sin(Y_0/150)$$

The standard error is 3.3 arc sec for yaw.

$$\text{Roll} = 26.0 + 0.9215R_0 + 0.0174P_0 + 0.5764 \times 10^{-4}R_0^2 + (0.6382)10^{-3}P_0^2 - (0.2471)10^{-3}R_0P_0 + (0.944)10^{-7}R_0^3 + (0.612)10^{-6}P_0^3 - (0.69)10^{-8}R_0P_0^2 - (0.181)10^{-6}R_0^2P_0 - 15.18(T_{OB1} - 23.6^\circ\text{C})$$

The standard error is 3.1 arc sec for roll.

Where P_0 = pitch output of the ATS

Y_0 = yaw output of the ATS

R_0 = roll output of the ATS

T_{OB1} = temperature of the optic bench ($^\circ\text{C}$) supporting the roll system optical head and base dihedral mirror.

The ATS performance verification in conjunction with the 20 ft long boom required considerable sophistication. A specially designed water tank flotation system was designed to simulate a zero gravity test condition. This included a precision pulley system to support each of the boom links from flotation rods suspended from the water tanks. The boom after being fully deployed was rotated through 360° in 90° steps for alignment measurement and the extrapolation of zero gravity attitude in all axes. Figure 15 is a sketch illustrating the test arrangement. As is evident from Fig. 15 there were a variety of mirrors 'M' attached to parts of the boom base and the instrument package for purposes of optical alignment and measurement in addition to reference mirrors and theodolite instrumentation. The spacecraft with the 20 ft long boom was equipped with a 3 axes gimbal at the boom base. This gimbal system provided a 2.5° range of adjustment of the boom attitude in each axis. The zero gravity boom gimbal angles were experimentally determined. The spacecraft was launched with these gimbal attitudes (which were pitch = $+7.5$ arc min.; yaw = $+10$ arc min.; roll = 32.5 arc min.).

Upon post-launch boom deployment in space, all three gimbals required adjustments of the order of 1 arc minute to bring the ATS into the near centre of its linear operating range in each axis. Optical acquisition was immediate with total fine adjustment completed within 24 hours after boom deployment.

ACKNOWLEDGEMENTS

This work was performed under sponsorship by NASA

Goddard Space Flight Center (Contract N00024-78-C-5384, Task I). The ATS was built by Barnes Engineering Company, Stamford, Conn., under the guidance of the Applied Physics Laboratory of the Johns Hopkins University. Mr. P. W. Collyer of BEC was the primary designer. The precision dihedral mirrors and plain mirrors were built by Muffaletto Optical Company, Baltimore, Maryland. Appreciation is expressed to R. R. Gardner of APL for the many long hours spent on the design and assistance in the operation of the water tank boom test flotation system.

NEW SPACE BOOKS

Remote Sensing of Earth from Space: Role of "Smart Sensors"
Ed. R. A. Breckenridge. American Institute of Aeronautics and Astronautics, 505 pp. 1979 \$22.50 (\$22.00 to AIAA members).

Remote sensing of the Earth has advanced enormously since, two decades ago, when the first Earth satellites returned simple radio transmissions and simple photographic information to ground receivers.

The resulting advances have been due largely to the result of big improvements in detection sensitivity, signal discrimination, and the introduction of new and more diverse sensors for different physical and chemical functions.

However, the basic remote sensing systems have, until now, remained essentially unaltered *viz* raw signals radioed to ground receivers where the electrical quantities are recorded, converted, computed and tabulated, etc.

The recent emergence of efficient detector arrays, microprocessors, integrated electronics, and specialised computer circuitry has sparked off a revolution in sensor system technology. This is the so-called "smart sensor" in the title of the book.

By incorporating many or all of the processing functions within the sensory device itself, a "smart sensor" has greater versatility and can extract much more useful information from the physical signals received, besides handling a much larger volume of data.

This is Vol. 67 in the AIAA series on Progress in Astronautics and Aeronautics.

Physics and Planetary Interiors

V. N. Zharkov and V. P. Trubitsyn. Pachart Publishing House, 388 pp. 1978, \$38.00.

This book was originally published in the USSR and has been translated and edited, with additional material provided, by W. B. Hubbard. Thus, to a large measure, the present book is based on research carried out in the Theoretical Physics Department of the USSR Academy of Sciences.

The first chapters deal with Geophysics, which include some modern Earth models and additional material concerned with viscosity and dissipation in the Earth's interior.

The final section of the book is particularly interesting. It is concerned with the interior structure of the planets, beginning with the origin, angular motion and distribution of the elements in the various bodies and leading to a description of how the Solar System might have originated and developed. This, in turn, leads to some of the fascinating problems of our time e.g. how did the Sun and planets form from a single interstellar cloud; how, indeed, did the planetary matter separate from the solar matter in the first place?

The remainder of the book continues by considering the interiors of the various major planets individually.

As might be expected, this is not a book for the general reader. Considerable knowledge of mathematics is required in order to follow some of the more intricate arguments.

Space Systems and their Interactions with Earth's Space Environment

Eds. H. B. Garrett and C. P. Pike. American Institute of Aeronautics and Astronautics, 737 pp. 1980.

This, Vol. 71 in the AIAA series "Progress in Astronautics and Aeronautics," presents a wide-ranging scientific examination of the many aspects of the interaction between space systems and the space environment, a subject of ever-growing importance in view of the more complicated missions now performed in space and the growing intricacy of spacecraft systems.

Among the many topics dealt with are changes in the upper atmosphere, the ionosphere, the plasmasphere and the magnetosphere, due to gas releases from large space vehicles, electrical charging of the spacecraft by the action of solar radiation and by interaction with the ionosphere and subsequent effects which may accrue, together with the effects of microwave beams, on the ionosphere. These include not only radiative heating but also electric breakdown of the surrounding gas, the creation of ionospheric "holes" and wakes by rapidly-moving spacecraft and other effects.

With such a diverse subject as this, the volume is necessarily interdisciplinary, so it will prove of value to physicists, communications engineers and scientists concerned with the upper atmosphere, as well as those concerned with the development of space vehicles generally.

Solar Flare Magnetohydrodynamics

Ed. E. R. Priest. Vol. 1. Gordon and Breach Science Publishers, 563 pp. 1981 \$89.50.

This is the first in a new series of books to be issued by the publishers on the general theme of the "Fluid Mechanics of Astrophysics and Geophysics."

Within the range of fluid mechanics, the two areas of astrophysics and geophysics have enjoyed increasing prominence. In the long term lies the problem of understanding and, possibly, controlling the Earth's atmosphere: in the shorter term, the questions of minimising harmful industrial waste and maximising agricultural yields. No less pressing is the development of the ocean resources and the need, therefore, to understand sea movements and how these can be harnessed.

Like Geomagnetism, most topics in Astrophysical Fluid Mechanics are hard to model in the laboratory. They include the study of Stellar Winds, the motion of Gas Clouds, Stellar Pulsation and Rotation, Magnetism and Star Formation by Gravitational Collapse.

The present volume includes a topic of particular significance at this time i.e. Solar Flares which release, in the space of an hour or so, an enormous quantity of energy which is then transformed into a complex variety of forms.

The present volume begins with description of such Flares and recent theories of their behaviour. It concentrates on the fundamentals of the Flare processes, particularly on their subsequent stability, magnetic configuration and how this energy is converted into heat and plasma energy.

Particle Acceleration is also considered extensively:

The result is an extensive study of the enormous advances in Solar Physics which have taken place recently, stemming not only from the use of high-resolution ground-based instruments but also from space telescopes, such as those on-board Skylab and the Solar Maximum Mission satellites.

**ATE
LME**